



Northern Illinois
University

Search for Charged Higgs Bosons in the $\tau + \ell$ Final State with 139 fb^{-1} of pp Collision Data at $\sqrt{s} = 13\text{ TeV}$ with the ATLAS Experiment

Dissertation Defense

Elliot Parrish

†Northern Illinois University, USA

October 13, 2022

Introduction

ATLAS

$$H^\pm \rightarrow \tau^\pm \nu_\tau$$

Theory

Fake Factors

The Standard Model

Background Modeling

Higgs Mechanism

MVA

BSM

PNN HPO

Charged Higgs Bosons

Systematic Uncertainties

Experimental Apparatus

Results

LHC

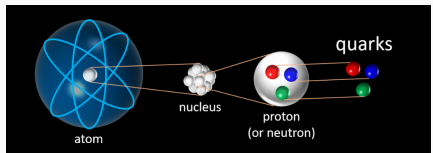
Conclusion

- This defense will take ~ 1 hour
 - I will walk you through the work that is contained in my PhD dissertation
 - After the presentation is complete, the committee and I will address comments privately
 - When we are done, I will return, the committee will discuss among themselves then return
- General Guidelines
 - Please remain muted unless you are speaking
 - There will be time at the end for questions, but feel free to interrupt if there is something urgent
- Thank you for attending!

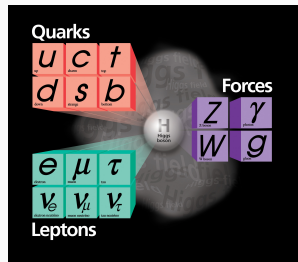
Theory

What are we made of?

- The scientific field of particle physics seeks to explain the building blocks of the universe
 - How many fundamental particles are there?
 - How do they interact with each other
- The Standard Model of Particle Physics (SM)
 - Matter is comprised of fermions
 - Quarks combine to create hadrons (protons, neutrons, $\pi^{\pm, 0}$, etc)
 - Anti-matter is identical to matter except for opposite electromagnetic charge
 - Forces are carried by an exchange of bosons
 - Gluon (g) → Strong force
 - Photon (γ) → Electromagnetism
 - W^\pm, Z^0 → Weak force



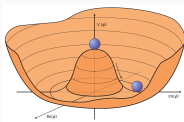
[1] [2]



The Higgs Mechanism



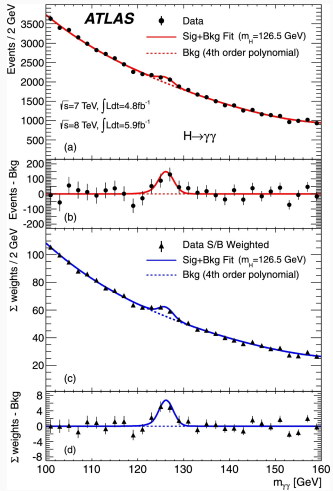
- Theorized by Higgs, Englert, and Brout in 1964
 - Complex scalar doublet ($s = 0$)
 - Non-zero vacuum expectation value
- Interactions with Higgs field give particles mass
- Discovered jointly by the ATLAS and CMS collaborations in 2012



Higgs potential [3]

Search for $H^\pm \rightarrow \tau^\pm \nu_\tau$ with ATLAS

Theory Higgs Mechanism



Higgs discovery [4]

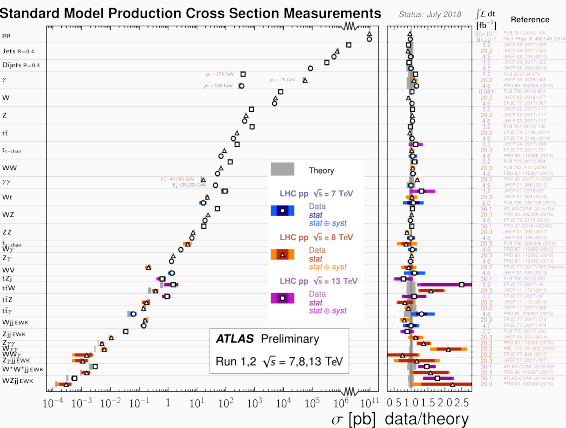
Elliot Parrish (NIU)

7 / 42

The Standard Model



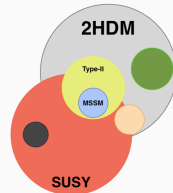
- Predicts the probabilities of particles decaying to others (among many other things)
 - Has been thoroughly tested
 - Measurements agree to a high degree of accuracy
 - Not a complete theory
 - Gravity
 - Matter-antimatter asymmetry in the universe
 - Predicted neutrino masses are 0
 - Observed neutrino mixing says otherwise



Beyond the Standard Model



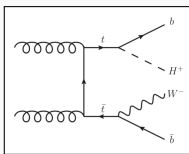
- Hierarchy problem, “unnaturalness”
 - Electroweak scale is ~ 100 GeV
 - Planck scale is $\sim 2.4 \times 10^{18}$ GeV
- 2 Higgs Doublet Models and Supersymmetry (SUSY) are large groups of theories
 - 2HDM have two complex doublet scalar fields [5]
 - Two relevant free parameters, $\tan \beta$ and m_{H^\pm}
 - $\tan \beta$ is the ratio of the vacuum expectation values of H^\pm
 - SUSY proposes a symmetry between fermions and bosons
 - Many new possible particles
 - Minimal Supersymmetric Standard Model (MSSM) is the smallest SUSY extension to the SM



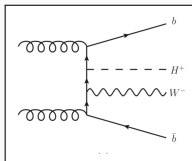
light neutral scalar	h^0
heavy neutral scalar	H^0
neutral pseudoscalar	A^0
two charged scalars	H^\pm

Charged Higgs Bosons

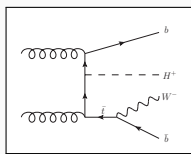
- At the LHC, theoretical production mode of m_{H^\pm} is mainly in top-quark decays or in association with a top-quark (t)
 - H^\pm production mode is dependent on m_{H^\pm}



$$m_{H^\pm} < m_t$$



$$m_{H^\pm} \simeq m_t$$



$$m_{H^\pm} > m_t$$

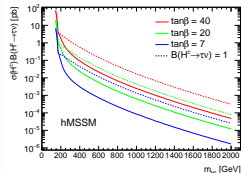
- $H^\pm \rightarrow \tau^\pm \nu_\tau$ decay channel remains significant for high $\tan \beta$
- Two sub-channels based on the decay mode of associated t

$t \rightarrow jets$

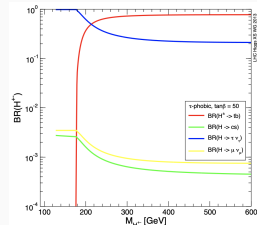
Sensitive at high mass due to higher $W \rightarrow q\bar{q}$ BR

$t \rightarrow \ell$

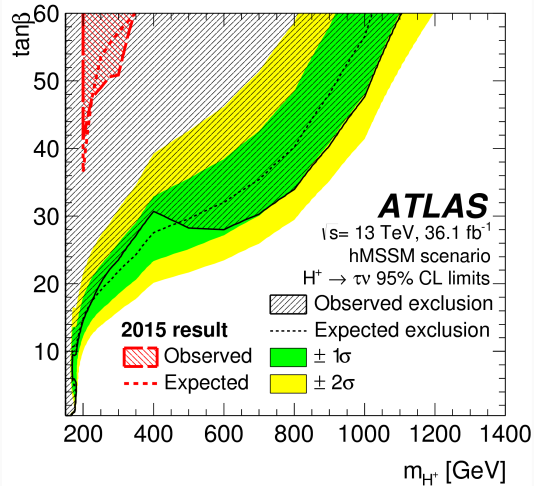
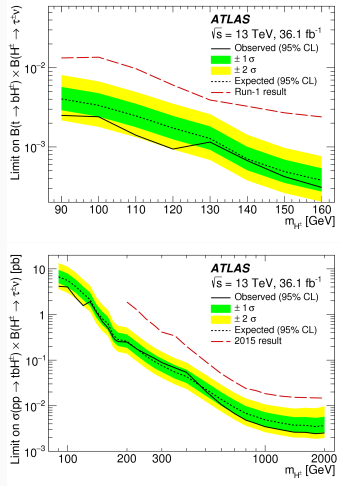
Sensitive at low mass due to easier triggering



[6]



[7]



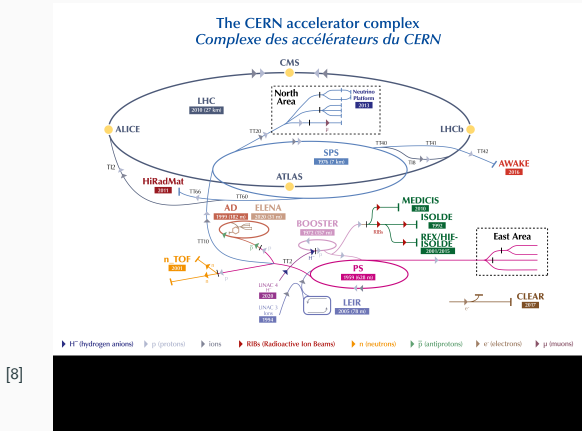
Experimental Apparatus

Large Hadron Collider



- Largest particle collider ever built
- Highest energy particle collider
- Located at CERN outside of Geneva, Switzerland
- Four main collision points
 - **ATLAS**, ALICE, CMS, LHCb

Circumference	26,659 m
Magnet operating temperature	1.9 K
Beam energy	6.5 TeV (13 CM TeV)
Protons per bunch	1.2×10^{11}
Bunches per beam	2808
Speed of bunches	> 1,000,000,000 km/hr ($\simeq 99.999\% c$)

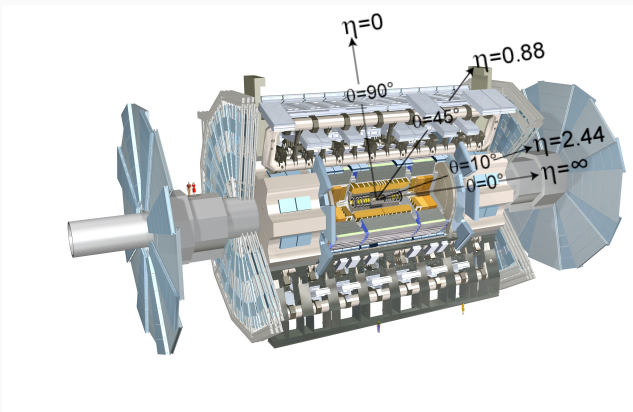


[9]

The ATLAS Detector



- General purpose particle detector
 - Magnet System
 - Tracker
 - Calorimeters
 - Muon Spectrometer
- Coordinate system origin at interaction point
 - r is radial distance
 - $\eta \equiv -\ln(\tan(\frac{\theta}{2}))$
 - ϕ is azimuthal angle
- Complex machine with
 $\sim 3,000$ scientific authors

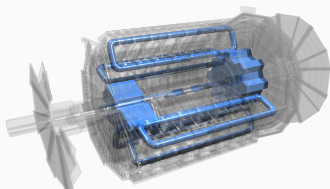


[10] [11]

Magnet System and Inner Detector

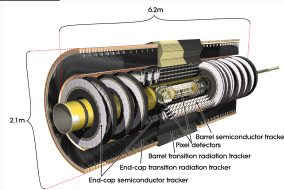
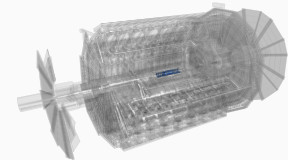
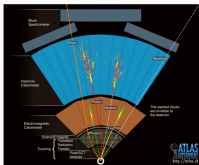


- Central solenoid
 - 2 T magnetic field
 - Bends charged particles in transverse plane
- Toroid system
 - 3.9 T magnetic field
 - Bends charged particles (μ) along beam axis



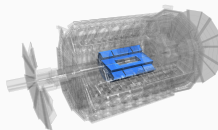
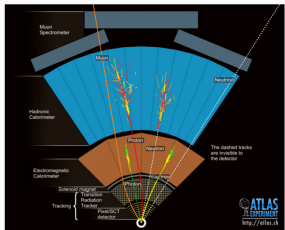
[10]

- Tracks trajectories of charged particles
 - Used to measure momentum in the transverse plane (p_T)

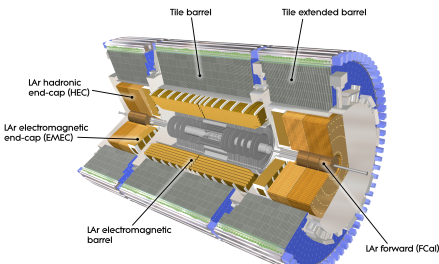


Calorimeters

- Measures energy of charged particles
 - Fully absorb particles
 - Liquid argon electromagnetic calorimeter
 - Scintillating tile hadronic calorimeter



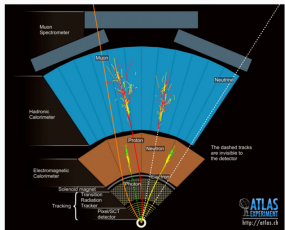
[10]



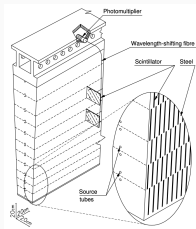
Tile Calorimeter



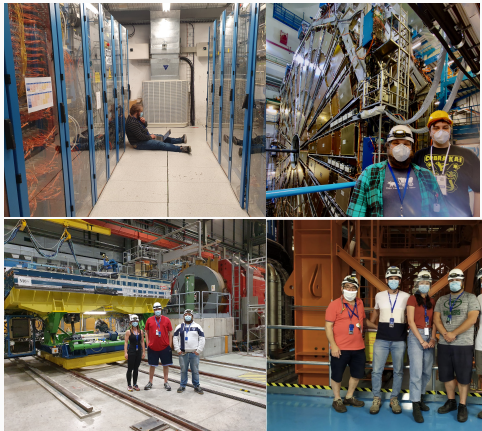
- Scintillating tile with steel absorber
- Important in jet, τ , E_T^{miss} and μ identification and triggering
- I served as Data Quality Co-Coordinator for several years
 - In Run-2 99.65% DQ efficiency [12]



Search for $H^\pm \rightarrow \tau^\pm \nu_\tau$ with ATLAS



Experimental Apparatus ATLAS



[13]

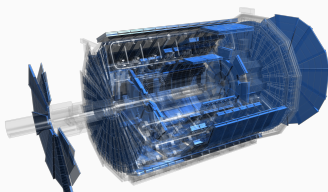
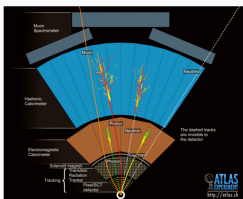
Elliot Parrish (NIU)

17 / 42

Muon System and Trigger



- Muon Spectrometers track trajectory of μ
 - Muons are minimally ionizing
 - μ reach the outermost region of the detector
- Information combined with inner detector to reconstruct μ

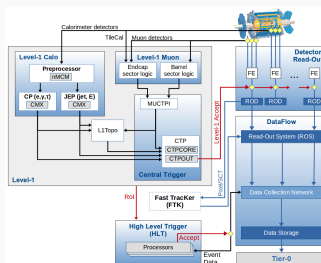


Search for $H^\pm \rightarrow \tau^\pm \nu_\tau$ with ATLAS

Experimental Apparatus ATLAS

Trigger System

- Need to quickly sort through data and decide if a collision is interesting or not
- Mix of hardware and software



[14]

Elliot Parrish (NIU)

18 / 42

$$H^\pm \rightarrow \tau^\pm \nu_\tau$$

Analysis Overview

- Search for singly charged H^\pm decaying to $\tau^\pm \nu_\tau$ over a wide mass range
 - Low mass ($m_{H^\pm} < m_t$):
 - Intermediate mass* ($m_{H^\pm} \simeq m_t$)
 - High mass ($m_{H^\pm} > m_t$)

- Dominant backgrounds

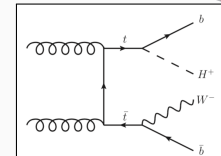
Backgrounds w/ prompt hadronic τ	Backgrounds w/ fake τ
---------------------------------------	----------------------------

$t\bar{t}$ estimated with MC	Fake $j \rightarrow \tau$ estimated with data driven fake factor method
$V + \text{jets}$ estimated with MC	Fake $\ell \rightarrow \tau$ estimated with MC, validated on $Z \rightarrow ee$
VV estimated with MC	

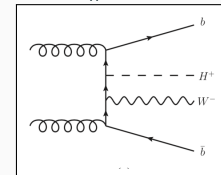
- MVA score is used as the final discriminant

Sub-Channel							
$\tau + \text{jets SR}$	E_T^{miss} Trigger	1 hadronic τ $p_T^\tau > 40$ GeV	0 ℓ (e or μ) $p_T^\ell > 20$ GeV	≥ 3 jets $p_T^j > 25$ GeV	≥ 1 b-jets $p_T^{b-jet} > 25$ GeV	$E_T^{\text{miss}} > 150$ GeV	$m_T(\tau, E_T^{\text{miss}}) > 50$ GeV
$\tau + \ell$ SR	Single Lepton Trigger	1 hadronic τ $p_T^\tau > 30$ GeV	1 ℓ (e or μ) $p_T^\ell > 30$ GeV	≥ 1 jet $p_T^j > 25$ GeV	≥ 1 b-jets $p_T^{b-jet} > 25$ GeV	$E_T^{\text{miss}} > 50$ GeV	Opposite sign τ and ℓ

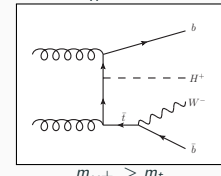
*: First time probed experimentally JHEP 09(2018)139



$$m_{H^\pm} < m_t$$



$$m_{H^\pm} \simeq m_t$$

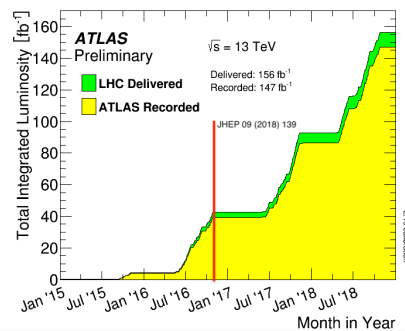


$$m_{H^\pm} > m_t$$

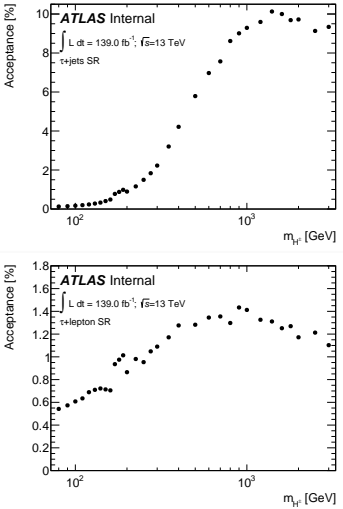
Updates to analysis since last publication



- Signal mass range extended
 - Previous: $90 \leq m_{H^\pm} \leq 2000$ GeV
 - Current: $80 \leq m_{H^\pm} \leq 3000$ GeV
- Signal filtering applied in order to effectively increase the statistics in the signal regions
- New analysis framework centered around using modern Machine Learning tools
- Investigated new multivariate analysis techniques
- Improved particle identification algorithms
- Almost 4× more data



Signal Acceptance



Background Estimation: $j \rightarrow \tau$ Fakes

- Extract Fake-Factors $FF = \frac{N_{\tau_{had-vis}}^{CR}}{N_{\bar{\tau}_{had-vis}}^{CR}}$ from two orthogonal control regions:

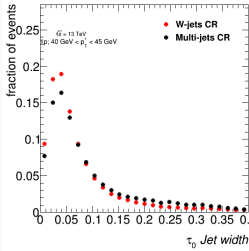
Multi-Jet (gluon enriched)	W+Jets (quark enriched)
E_T^{miss} or Multi-Jet trigger	Single lepton triggers
$\geq 1\tau_{had}, p_T > 30 \text{ GeV}$	$\geq 1\tau_{had}, p_T > 30 \text{ GeV}$
$\geq 3 \text{ jets}$	$\geq 1 \text{ jet}$
0 b-jets	0 b-jets

- Combine the two Fake-Factors via the template fit method:
 - Find two separate templates for anti- τ in each CR
 - Fit both templates to the shape of the anti- τ in the SR
 - Lowest χ^2 of the fit defines α_{MJ} value and the corresponding error

$$FF_i^{\text{comb}} = \alpha_i^{MJ} FF_i^{MJ} + [1 - \alpha_i^{MJ}] FF_i^{W+jets}$$

- Number of events with fake τ in the signal region is given by:

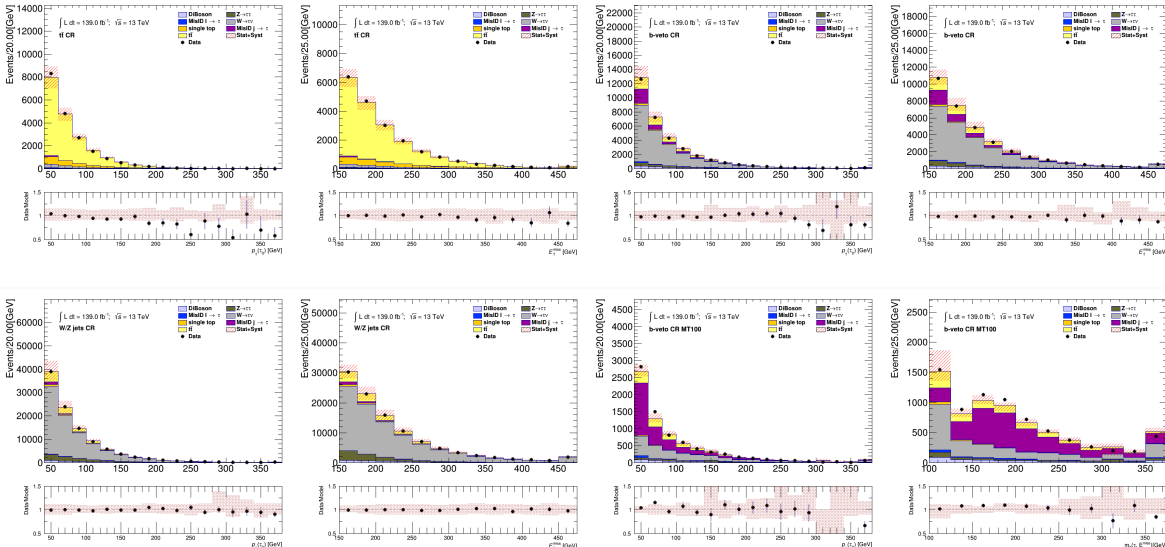
$$N_{\text{fakes}}^{\tau_{had-vis}} = \sum_i N_{\bar{\tau}_{had-vis}}^{SRi} FF_i$$



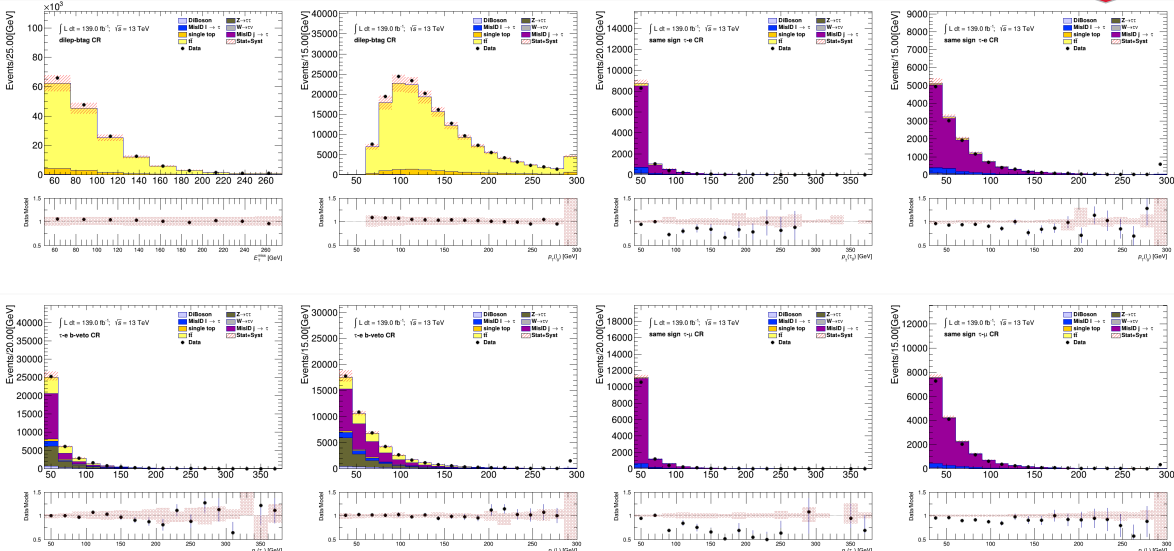
- $\bar{\tau}_0$ jet width used in α fitting of 1-prong and 3-prong $\bar{\tau}$

$\bar{\tau} ID$
RNN Score > 0.01
Not loose

$\tau + \text{jets}$ Background Modeling



$\tau + \ell$ Background Modeling

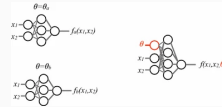


- Boosted Decision Tree (BDT)
 - Excel at exploiting linear correlations
 - Often combined into a random forest
- Neural Networks
 - Excel at exploiting non-linear correlations

Parameterized Neural Networks



- Background modeling and classifier training kept statistically independent via the k-fold method
 - For this analysis $k = 5$
- Trained using MC for backgrounds with true τ
- Data-driven $j \rightarrow \tau$ fakes included for ≥ 500 GeV
- Parameterized Neural Networks (PNNs) can be trained and evaluated on an entire mass range
 - Detailed information here: [arXiv:1601.07913](https://arxiv.org/abs/1601.07913)
- Separate models trained on 1 prong and 3 prong τ
- $\tau + \ell$ channel is trained inclusive for $\tau + e$ and $\tau + \mu$



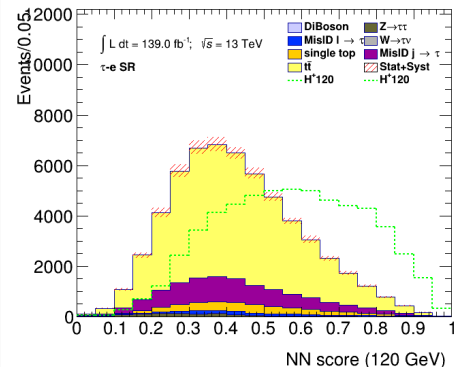
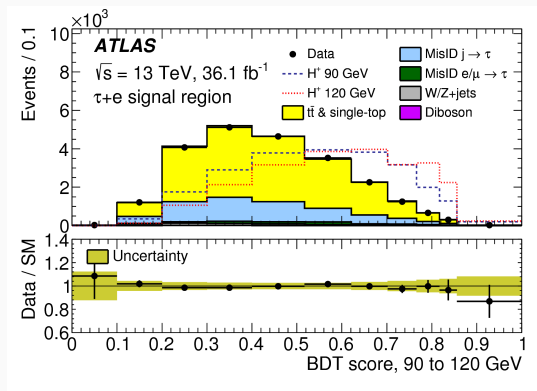
[15]

	Field 1	Field 2	Field 3	Field 4	Field 5	Background
Partition 1	Evaluation	Train	Evaluation	Train	Evaluation	Train
Partition 2	Train	Evaluation	Train	Evaluation	Train	Evaluation
Partition 3	Train	Evaluation	Train	Evaluation	Train	Evaluation
Partition 4	Train	Evaluation	Train	Evaluation	Train	Evaluation
Partition 5	Train	Evaluation	Train	Evaluation	Train	Evaluation

$\tau + \ell$ Input Variables		
p_T^τ	η^τ	ϕ^τ
p_T^ℓ	η^ℓ	ϕ^ℓ
$p_T^{j_0}$	η^{j_0}	ϕ^{j_0}
E_T^{miss}	$\phi^{E_T^{\text{miss}}}$	$p_T^{j_1}$
$m_{Truth}^{H^\pm}$	Υ^τ	

$\tau + \text{jets}$ Input Variables		
p_T^τ	η^τ	ϕ^τ
$p_T^{j_0}$	η^{j_0}	ϕ^{j_0}
$p_T^{j_1}$	η^{j_1}	ϕ^{j_1}
$p_T^{j_2}$	η^{j_2}	ϕ^{j_2}
E_T^{miss}	$\phi^{E_T^{\text{miss}}}$	$m_{Truth}^{H^\pm}$

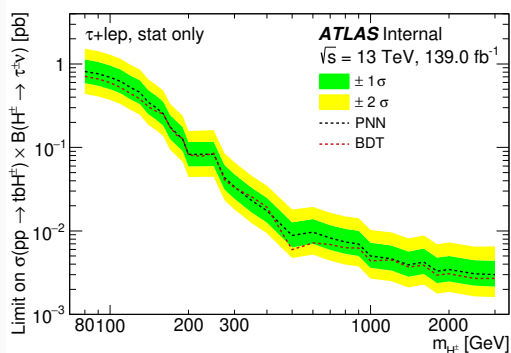
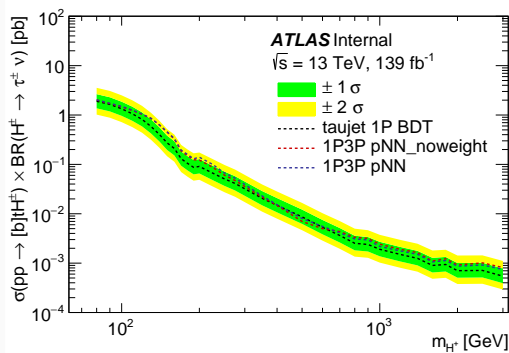
Boosted Decision Tree vs Parameterized Neural Network



Boosted Decision Tree vs Parameterized Neural Network



- One model for entire mass range makes analysis less computationally expensive
- PNN can be evaluated on mass points that are not simulated
- Limits are preliminary, many fixes and changes have been implemented since



PNN Input Variable Selection



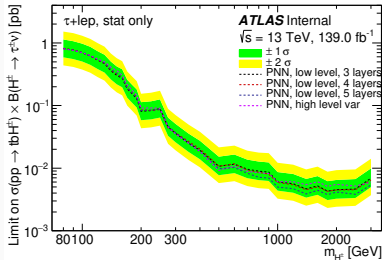
Low Level Input Variables

p_T^τ	η^τ	ϕ^τ
p_T^ℓ	η^ℓ	ϕ^ℓ
p_T^{b-jet}	η^{b-jet}	ϕ^{b-jet}
p_T^{jet}	η^{jet}	ϕ^{jet}
E_T^{miss}	ϕ_E^{miss}	$p_T^{j_1}$
Υ	$m_{H^\pm}^{\text{Truth}}$	

High Level Input Variables

p_T^τ	p_T^{b-jet}	p_T^ℓ
E_T^{miss}	$\Delta\phi_{\tau, \text{miss}}$	$\Delta\phi_{b-jet, \text{miss}}$
$\Delta\phi_{\ell, \text{miss}}$	$\Delta R_{\tau, \ell}$	$\Delta R_{b-jet, \ell}$
$\Delta R_{b-jet, \tau}$	$\Delta\phi_{\tau, \text{miss}}/\Delta\phi_{\text{jet}, \text{miss}}$	Υ
$m_{H^\pm}^{\text{Truth}}$		

- Comparison between raw input variables and engineered variables
- Expected limits in the $\tau + \ell$ subchannel was used as figure of merit
- Low level variables best at high m_{H^\pm}



PNN Hyperparameter Optimization



- Performed in the $\tau + \ell$ sub-channel
- Used area under curve (AUC) of scores as figure of merit
 - Averaged over 5 kfolds, standard deviation is taken from kfolds
- Used early stopping for training
 - $\Delta_{min} = 0.00001$ and a patience of 10
 - Best weights were kept
- To make hyperparameter optimization (HPO) go quicker, ran multiple small grids of hparams
 - Scan over activation functions and loss functions
 - Scan over dropout value
 - Scan over activation function
 - Scan over LeakyReLU α
 - Fixed alpha over more widths and depths
 - AUC from 80 GeV to 500 GeV to optimize for low mass

- LeakyReLU activation function has an α parameter
- Slope of negative portion
 - Prevents neurons from "dying" by allowing negative weight values
- Standard relu is where $\alpha = 0$



PNN Hyperparameter Optimization



Parameter			
activation function	softsign	relu	LeakyReLU
loss function	binary crossentropy	mean squared error	mean absolute error
width	32		
depth	10		

Parameter			
width	8	16	32
depth	3	5	10
dropout	0.1	0.3	
activation function	softsign		
loss function	binary crossentropy		

Parameter			
width	32	64	128
depth	2	3	4
dropout	0.1		
activation function	softsign	relu	LeakyReLU
batch size	1025		
loss function	binary crossentropy		

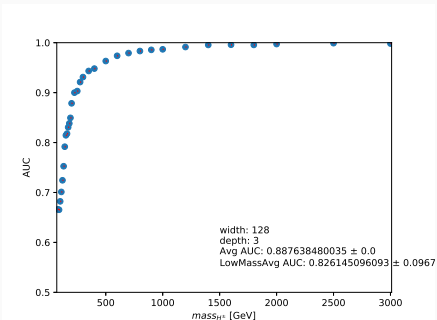
Parameter				
width	32	64	128	
depth	2	3	4	
α	0.01	0.05	0.001	0.005
batch size	1024			
dropout	0.1			
activation function	LeakyReLU			
loss function	binary crossentropy			

Parameter				
width	32	64	128	256
depth	2	3	4	5
batch size	1024			
dropout	0.1			
activation function	LeakyReLU			
α	0.05			
loss function	binary crossentropy			

Final PNN Model Performance



width	depth	Avg	LowMassAvg
128	3	0.8876 ± 0.0000	0.8261 ± 0.0968
128	5	0.8861 ± 0.0000	0.8235 ± 0.1000
128	4	0.8858 ± 0.0000	0.8232 ± 0.0994
128	2	0.8857 ± 0.0000	0.8231 ± 0.1006
64	4	0.8857 ± 0.0002	0.8230 ± 0.0994
64	2	0.8855 ± 0.0004	0.8228 ± 0.0996
64	5	0.8853 ± 0.0005	0.8224 ± 0.0997
64	3	0.8853 ± 0.0011	0.8223 ± 0.0994
256	5	0.8844 ± 0.0002	0.8213 ± 0.1003
256	4	0.8823 ± 0.0000	0.8181 ± 0.1013
32	3	0.8798 ± 0.0012	0.8139 ± 0.1031
32	4	0.8799 ± 0.0009	0.8139 ± 0.1031
32	2	0.8796 ± 0.0004	0.8135 ± 0.1023
32	5	0.8792 ± 0.0011	0.8128 ± 0.1035
256	2	0.8781 ± 0.0002	0.8120 ± 0.1023



Fake-factor method uncertainties



Sources of systematic uncertainties associated with the FF method:

- Statistical uncertainties
- True τ contamination in the anti- τ CR
- α_{MJ} fitting procedure uncertainty
- Smirnov transformation
- Tau RNN Identification SF variation
- Heavy flavor jet fraction

Source of uncertainty	$\tau + \text{jets}$		$\tau + \ell$	
	Effect on yield	Shape	Effect on yield	Shape
Fake factors: statistical uncertainties	3.9%	✗	3.2%	✗
Fake factors: True $\tau_{\text{had-vis}}$ in the anti- $\tau_{\text{had-vis}}$ CR	+3.4% -3.2%	✗	+4% -4.3%	✗
Fake factors: tau RNN Identification SF	2.7%	✓	2.7%	✓
Fake factors: α_{MJ} uncertainty	3.6%	✗	1.9%	✗
Fake factors: Smirnov transform	0%	✓	0%	✓
Fake factors: heavy flavor jet fraction	6%	✓	5.53%	✓

Sources of Systematic Uncertainty

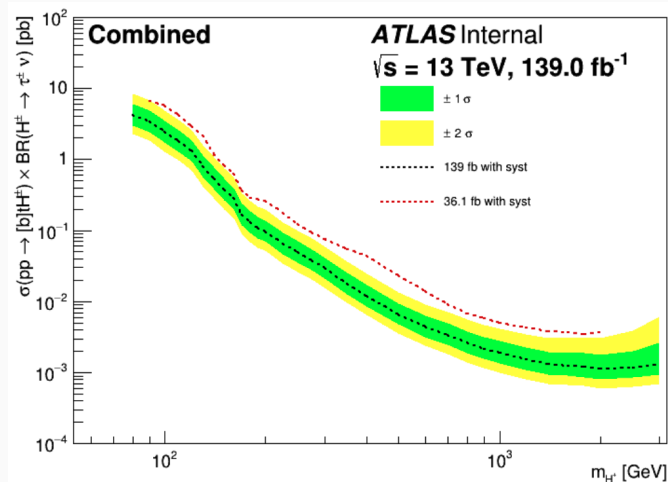


Table with sys

Expected Yields



$H^\pm \rightarrow \tau\nu$ Expected Limits



Combined

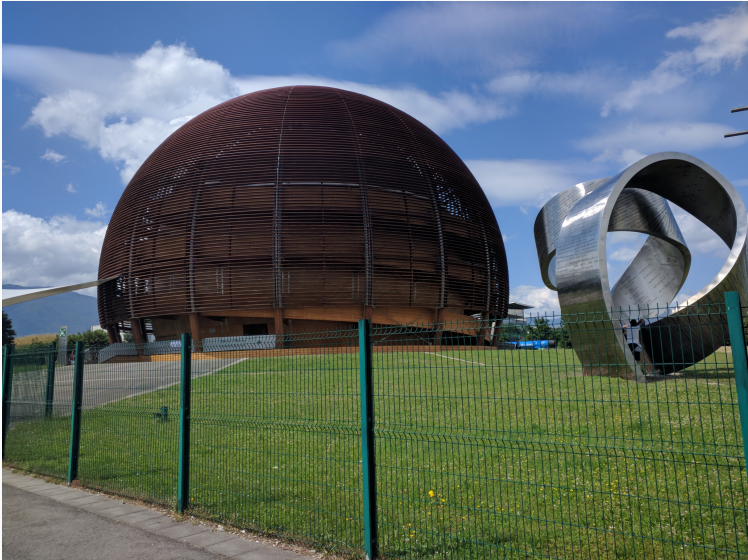
Conclusion

Conclusions



- New analysis strategy outperforms previous analysis by a factor of XX
- Analysis is still blinded
- Paper will be published soon

Thank You



Bibliography

References i

- [1] D. Hemphill, *The behavior of the primordial universe*, Apr. 2020. [Online]. Available:
https://www.physics.purdue.edu/about/prizes_awards/charlotte_ida_litman_tubis_award/2017_behavior_primordial_universe.html.
- [2] D. Leah, *The standard model: The most successful theory ever*, Jul. 2016. [Online]. Available: <https://news.fnal.gov/2011/11/the-standard-model-the-most-successful-theory-ever/>.
- [3] J. Ellis, “Higgs Physics,” 117–168. 52 p, Dec. 2013, 52 pages, 45 figures, Lectures presented at the ESHEP 2013 School of High-Energy Physics, to appear as part of the proceedings in a CERN Yellow Report. DOI: 10.5170/CERN-2015-004.117. arXiv: 1312.5672. [Online]. Available: <https://cds.cern.ch/record/1638469>.

References ii

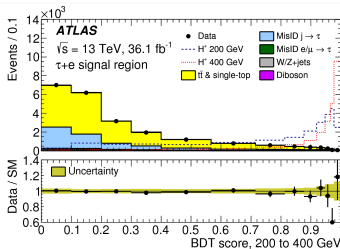
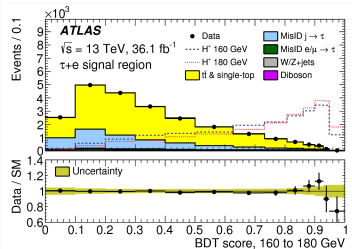
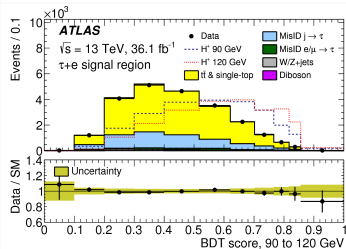
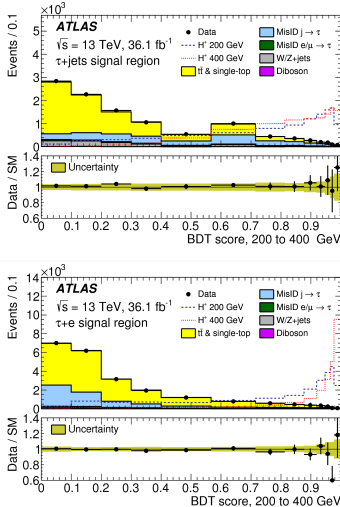
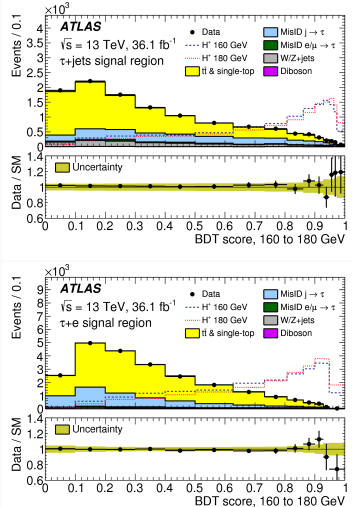
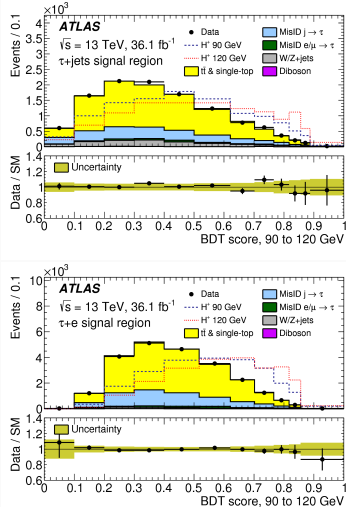
- [4] ATLAS Collaboration, "Observation of a new particle in the search for the standard model higgs boson with the atlas detector at the lhc," *Physics Letters B*, vol. 716, no. 1, pp. 1–29, 2012.
- [5] G. Branco, P. Ferreira, L. Lavoura, M. Rebelo, M. Sher, and J. P. Silva, "Theory and phenomenology of two-higgs-doublet models," *Physics Reports*, vol. 516, no. 1–2, pp. 1–102, Jul. 2012, ISSN: 0370-1573. DOI: 10.1016/j.physrep.2012.02.002. [Online]. Available: <http://dx.doi.org/10.1016/j.physrep.2012.02.002>.
- [6] The ATLAS Collaboration, "Search for charged Higgs bosons decaying via $H^\pm \rightarrow \tau^\pm \nu_\tau$ in the $\tau + \text{jets}$ and $\tau + \text{lepton}$ final states with 36 fb^{-1} of pp collision data recorded at $\sqrt{s} = 13 \text{ TeV}$ with the ATLAS experiment," *JHEP*, vol. 09, p. 139, 2018. DOI: 10.1007/JHEP09(2018)139. arXiv: 1807.07915 [hep-ex].

References iii

- [7] C. T. Potter, H. Mantler, S. Lehti, I. Puljak, H. Kim, R. Klees, D. De Florian, R. K. Ellis, S. Frixione, J. Thompson, J. Huston, S. Y. Choi, D. Rebuzzi, M. Schulze, J. Yu, R. Rietkerk, R. Di Nardo, M. Zaro, R. Harlander, S. Dittmaier, C. Oleari, A. David, F. Maltoni, L. Kashif, B. Di Micco, M. V. Acosta, P. T. E. Taylor, S. O. Moch, J. Olsen, S. Bolognesi, G. Weiglein, M. Ubiali, M. Rauch, F. J. Tackmann, D. Wackerloha, N. V. Tran, Y. Gao, M. Muhlleitner, P. Vanlaer, X. Liu, A. Whitbeck, M. Zanetti, T. Peraro, D. Del Re, G. Degrassi, J. M. Smillie, P. Monni, E. Mirabella, F. Schissler, K. Mawatari, D. Tommasini, P. Torrielli, S. Heinemeyer, P. Govoni, P. Slavich, M. Kramer, G. Sborlini, R. Tanaka, R. Hernandez-Pinto, J. R. Walsh, G. Passarino, C. Zhang, C. Wagner, G. Ferrera, Z. Trocsanyi, C. Mariotti, G. P. Salam, B. Mellado, M. Kadastik, D. Gillberg, T. J. E. Zirke, F. Krauss, A. Rizzi, P. Bolzoni, Q. Li, C. Neu, M. Schonherr, T. Becher, M. Grazzini, P. Musella, M. Carena, M. V. Garzelli, E. A. Bagnaschi, A. Kardos, W. J. Walsh, II, Q. Si, J. J. M. Gritsch, D. G. Hull, D. J. Miller, D. R.

Backup

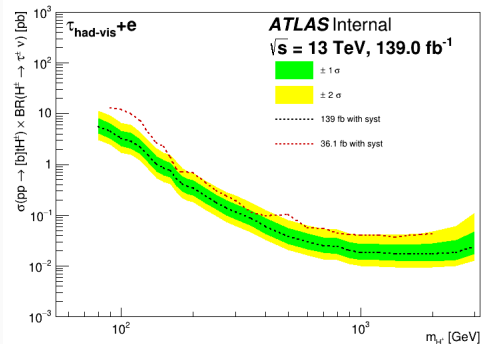
JHEP 09(2018)139 BDT Scores in Signal Regions



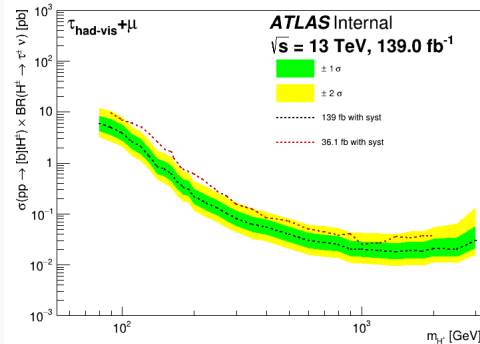
PNN Hyperparameter Optimization Results

width	depth	80	150	250	500	Avg	LowMassAvg
128	3	0.6661 ± 0.0000	0.8145 ± 0.0000	0.9031 ± 0.0000	0.9633 ± 0.0000	0.8876 ± 0.0000	0.8261 ± 0.0968
128	5	0.6492 ± 0.0000	0.8043 ± 0.0000	0.9078 ± 0.0000	0.9628 ± 0.0000	0.8861 ± 0.0000	0.8235 ± 0.1000
128	4	0.6593 ± 0.0000	0.8117 ± 0.0000	0.9012 ± 0.0000	0.9638 ± 0.0000	0.8858 ± 0.0000	0.8232 ± 0.0994
128	2	0.6444 ± 0.0000	0.8070 ± 0.0000	0.9075 ± 0.0000	0.9631 ± 0.0000	0.8857 ± 0.0000	0.8231 ± 0.1006
64	4	0.6576 ± 0.0050	0.8080 ± 0.0013	0.9052 ± 0.0045	0.9656 ± 0.0016	0.8857 ± 0.0002	0.8230 ± 0.0994
64	2	0.6528 ± 0.0066	0.8052 ± 0.0023	0.9057 ± 0.0032	0.9651 ± 0.0007	0.8855 ± 0.0004	0.8228 ± 0.0996
64	5	0.6538 ± 0.0050	0.8044 ± 0.0019	0.9058 ± 0.0037	0.9653 ± 0.0014	0.8853 ± 0.0005	0.8224 ± 0.0997
64	3	0.6520 ± 0.0067	0.8051 ± 0.0018	0.9042 ± 0.0044	0.9649 ± 0.0019	0.8853 ± 0.0011	0.8223 ± 0.0994
256	5	0.6536 ± 0.0010	0.8044 ± 0.0033	0.9036 ± 0.0042	0.9644 ± 0.0022	0.8844 ± 0.0002	0.8213 ± 0.1003
256	4	0.6434 ± 0.0000	0.8018 ± 0.0000	0.9017 ± 0.0000	0.9619 ± 0.0000	0.8823 ± 0.0000	0.8181 ± 0.1013
32	3	0.6369 ± 0.0094	0.7950 ± 0.0041	0.8977 ± 0.0032	0.9635 ± 0.0022	0.8798 ± 0.0012	0.8139 ± 0.1031
32	4	0.6384 ± 0.0037	0.7935 ± 0.0033	0.8986 ± 0.0037	0.9636 ± 0.0016	0.8799 ± 0.0009	0.8139 ± 0.1031
32	2	0.6399 ± 0.0058	0.7924 ± 0.0024	0.8983 ± 0.0033	0.9629 ± 0.0023	0.8796 ± 0.0004	0.8135 ± 0.1023
32	5	0.6350 ± 0.0077	0.7931 ± 0.0056	0.8981 ± 0.0022	0.9625 ± 0.0005	0.8792 ± 0.0011	0.8128 ± 0.1035
256	2	0.6320 ± 0.0044	0.7971 ± 0.0000	0.8939 ± 0.0034	0.9587 ± 0.0018	0.8781 ± 0.0002	0.8120 ± 0.1023

$H^\pm \rightarrow \tau\nu$ Expected Limits

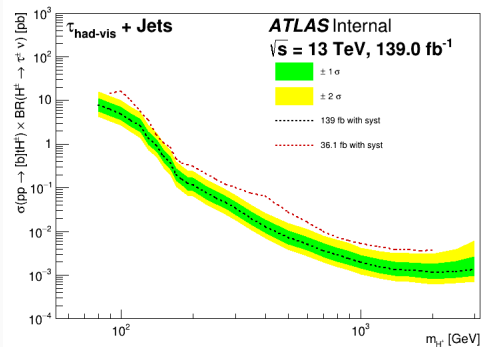


$\tau + e$

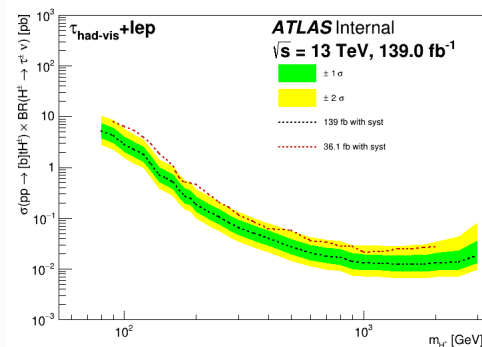


$\tau + \mu$

$H^\pm \rightarrow \tau\nu$ Expected Limits



$\tau + jets$



$\tau + \ell$